

APPENDIX D

Computation of the WSPRO Discharge Coefficient and Effective Flow Length

This appendix documents how the effective flow length and discharge coefficient are computed for the WSPRO bridge hydraulics methodology in HEC-RAS. The effective flow length is used in the computation of friction losses from the cross section just upstream of the bridge (section 3) to the approach cross section (section 4). The coefficient of discharge is used in the expansion loss equation from sections 1 to 2. The information in this appendix was extracted directly from the Federal Highway Administrations Research Report entitled: “Bridge Waterways Analysis Model” (FHWA, 1986).

Effective Flow Length

Since friction losses are directly proportional to flow length, it becomes imperative to obtain the best possible estimate of flow length, especially for those cases where the friction loss is a significant component of the energy balance between two sections. For minor degrees of constriction, a straight line distance between cross sections is usually adequate. However, for more significant constrictions, this straight-line distance is representative of only that portion of the flow that is generally in direct line with the opening. Flow further away from the opening must flow not only downstream, but also across the valley to get to the opening, thus traveling much farther than the straight-line distance.

Schneider et al. (USGS, 1977) tabulated average streamline lengths for various approach section locations and various degrees of constriction. These results are not directly applicable in this model because they are derived for symmetric constrictions in channel reaches having uniform, homogeneous flow conveyance characteristics. Even if the exact-solution algorithms were developed for non-symmetric, non-homogeneous conditions, the computer resource requirements for an exact solution are too great to warrant inclusion in the model. Therefore, a simplified computational technique was developed and incorporated into the model to compute average streamline length.

Schneider et al., defined the optimum location of the approach section as:

$$L_{opt} = \frac{b}{\pi(1 - m')} \phi \quad (D-1)$$

Where L_{opt} is the distance, in ft, between the approach section and the

upstream face of the bridge opening, b is the bridge-opening width, and m' is the geometric contraction ratio computed by:

$$m' = 1 - \frac{b}{B} \quad (D-2)$$

Where B is the top width, in ft, of the approach section flow area. The Φ term in equation D-1 is computed by:

$$\phi = \frac{1}{2} \ln \left[\left(\sqrt{\frac{8}{\varepsilon^2} + 8} - \frac{3}{\varepsilon} - \varepsilon \right) \left(\sqrt{8 + 8\varepsilon^2} - 3\varepsilon - \frac{1}{\varepsilon} \right) \right] - \ln \left(\varepsilon - \frac{1}{\varepsilon} \right) \quad (D-3)$$

Where ε is computed by:

$$\varepsilon = 1 + \delta + \sqrt{\delta^2 + 2\delta} \quad (D-4)$$

With δ computed as:

$$\delta = \frac{2}{\tan^2 \left[\left(1 - \frac{b}{2B} \right) \pi \right]} \quad (D-5)$$

L_{opt} is located in a zone of nearly one-dimensional flow, thus satisfying the basic requirements of the one-dimensional energy equation.

The simplified computational technique varies depending upon the relative magnitudes of L_{opt} and b . To introduce the technique, discussion is limited to the ideal situation of a symmetric constriction with uniform, homogeneous conveyance. For such conditions only one-half of the valley cross-section is required. This one-half section is divided into ten equal conveyance stream tubes between edge of water and the centerline at both the L_{opt} location and the upstream face of the bridge. Equal-conveyance stream tubes are equivalent to equal-flow stream tubes for one-dimensional flow. Figure D.1 illustrates a case with a small geometric contraction ratio. L_{opt} is less than b for lesser degrees of constriction. Since L_{opt} is located in a zone of nearly one-dimensional flow, the streamlines are essentially parallel between the approach section and the L_{opt} location. Between L_{opt} and the bridge opening the corresponding flow division points are connected with straight lines. The effective flow length used by the model is the average length of the ten equal-flow stream tubes computed by:

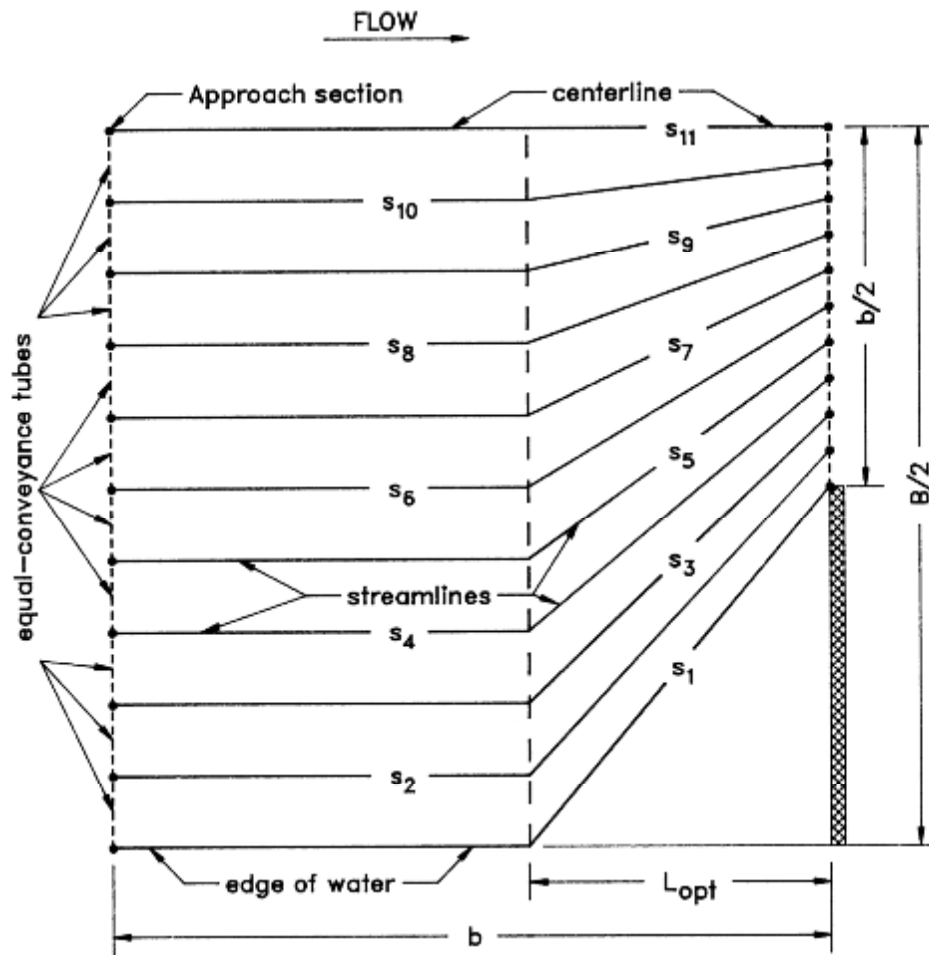


Figure D.1. Definition sketch of assumed streamlines for relatively low degree of contraction.

$$L_{av} = \frac{1}{10} \left[\sum_{i=2}^{10} S_i + \frac{(S_1 + S_{11})}{2} \right] \quad (D-5)$$

Where i indicates the streamline number and s is the individual streamline length. Although the straight-line pattern is a gross simplification of the actual curvilinear streamlines, the computed L_{av} values are less than 2 percent smaller than the exact solution for small geometric contraction ratios.

Figure D.2 illustrates a relatively high degree of geometric contraction. Simply connecting the flow division points of the L_{opt} and bridge sections does not result in representative lengths for those streamlines furthest away from the opening.

Therefore, a parabola is computed by the equation:

$$y^2 = 2b \left(x + \frac{b}{2} \right) \quad (D-6)$$

This parabola has its focus at the edge of water and its axis in the plane of the upstream face of the bridge. Positive x and y distances are measured from the edge of water towards the stream centerline and upstream from the plane of the bridge, respectively. For portions of the section where L_{opt} is upstream from this parabola, the parallel streamlines are projected to the parabola and then a straight line connects this projected point with the corresponding flow division point in the bridge opening. Flow division points of the L_{opt} section at or downstream from the parabola are connected directly to their corresponding flow division point for the bridge opening. Only the distances between the approach and the cross section just upstream of the bridge opening are used to compute L_{av} with equation D-5. This process generally produces results that are within 5 percent of the exact solution. For very severe constrictions (i.e., $m' = 0.95$), the differences are closer to 10 percent.

The non-uniform conveyance distribution in the approach reach is represented by defining the stream tubes on a conveyance basis. The model determines the horizontal stationing of 19 interior flow division points that subdivide both the L_{opt} and bridge sections into 20 tubes of equal conveyance. Asymmetric constrictions with nonuniform conveyances are analyzed by treating each half of the reach on either side of the conveyance midpoints separately, then averaging the results. L_{av} for each side provides the conveyance-weighted average streamline length. Figure D.3 illustrates a typical asymmetric, nonuniform conveyance situation.

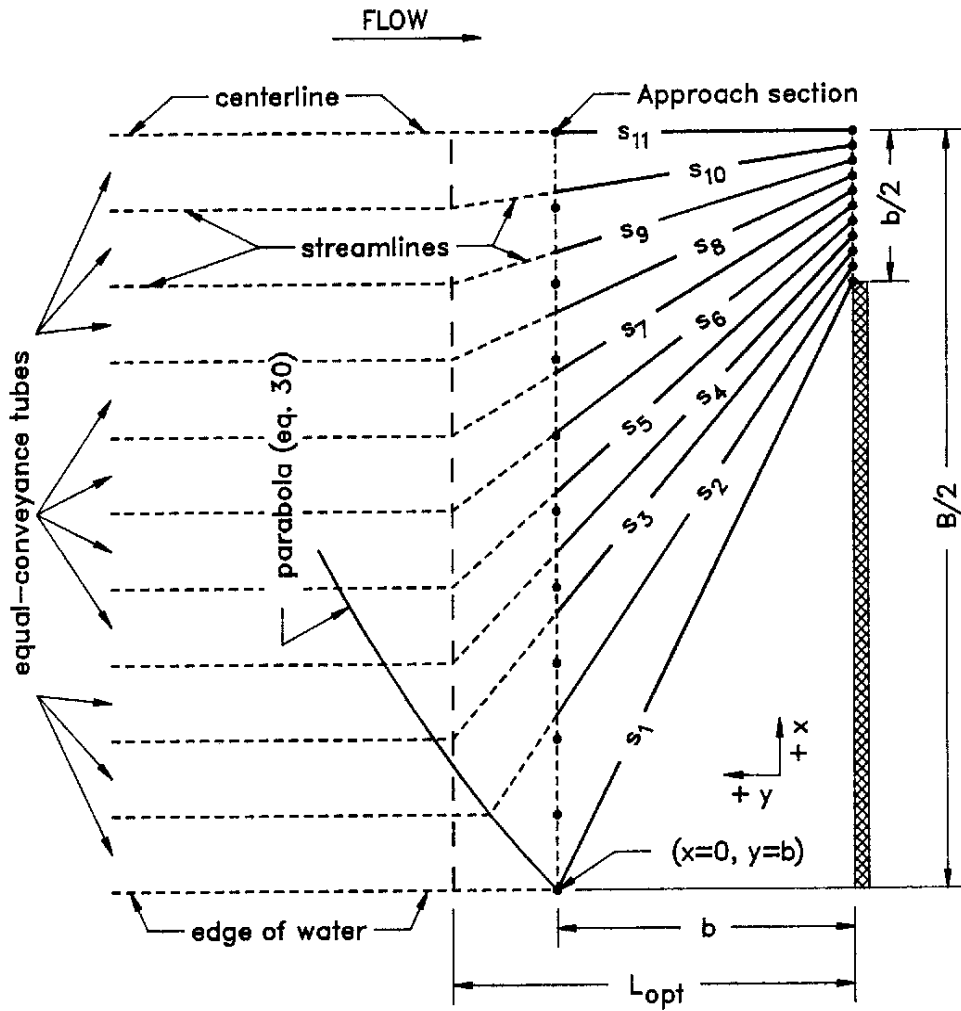


Figure D.2. Definition sketch of assumed streamlines for relatively high degrees of contraction.

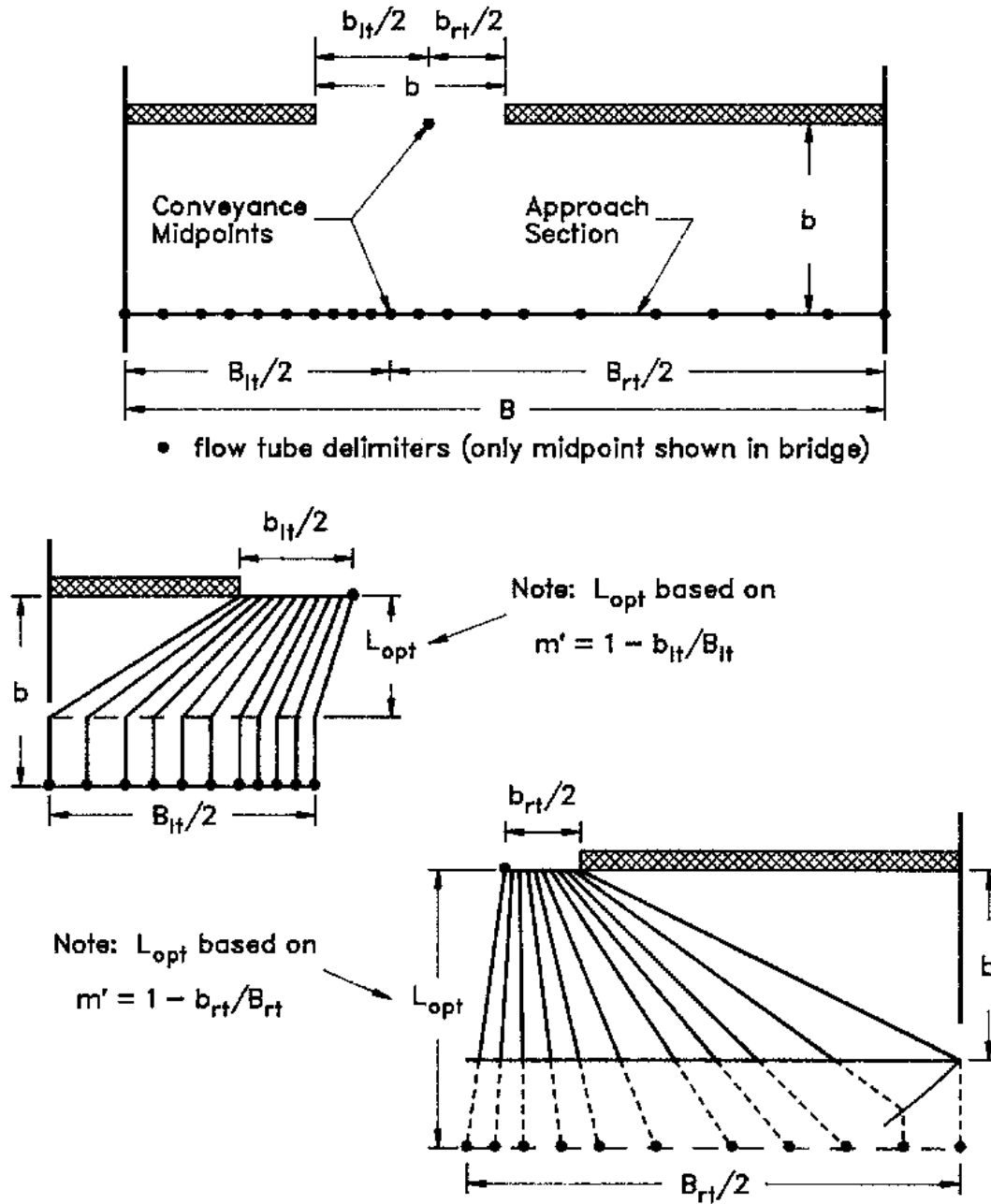


Figure D.3. Assumed flow pattern for a nonsymmetric constriction with nonhomogenous roughness distribution.

Coefficient of Discharge

The coefficient of discharge, as defined by Matthai and used in this model, is a function of bridge geometry and flow characteristics. Matthai's report presents detailed instructions for computing the coefficient of discharge for the four most common types of bridge openings. It is not practical to reproduce that entire report herein, but the following paragraphs summarize the procedures as adapted to this model. All of the key figures from Matthai's report, the tabular values and equations used to determine the coefficient of discharge, and a discussion of the minor modifications made to Matthai's procedures are presented in this appendix. Bridge openings are classified as one of four different types depending upon characteristics of embankment and abutment geometry. Regardless of opening type, the first step is to determine a base coefficient of discharge, C' , which is a function of (1) a channel contraction ratio and (2) a ratio of flow length through the bridge, L , to the bridge-opening width, b . The channel contraction ratio is

$$m = 1 - \frac{K_q}{K_1} \quad (D-7)$$

Where K_q is the conveyance of a portion of the approach section (based on projecting the bridge opening width up to the approach section) and K_1 is the total conveyance of the approach section. The definition of the L and b terms for the length ratio depends upon the opening type. The definition sketches below define these terms for each opening type. The final coefficient of discharge, C , is computed by multiplying C' by a series of adjustment factors to account for variations in geometry and flow from the base conditions used to derive C' . The number of parameters for which adjustment factors are required depends partially upon the opening type. Following is a summary description of the opening types and the adjustment factors that are unique to each:

- Type 1 openings have vertical embankments and vertical abutments with or without wingwalls. The discharge coefficient is adjusted for the Froude number (k_f) and also for wingwall width (k_w) if wingwalls are present or for entrance rounding (k_r) if there are no wingwalls.
- Type 2 openings have sloping embankments and vertical abutments and do not have wingwalls. The discharge coefficient is adjusted on the basis of the average depth of flow at the abutments (k_y).
- Type 3 openings have sloping embankments with spillthrough abutments. The discharge coefficient is adjusted on the basis of entrance geometry (k_x).
- Type 4 openings have sloping embankments, vertical abutments, and wingwalls. The discharge coefficient is adjusted depending upon the wingwall angle (k_θ).

In addition to the above adjustment factors, which are dependent upon opening type, there are adjustment factors for piers or piles (k_j) and spur dikes (k_a, k_b, k_d) that may be applied to all opening types. The relationships used to compute all of the above adjustment factors are shown below.

Figures D.4 through D.7 are definition sketches of the four types of openings for which Matthai defined the coefficient of discharge. Figures D.8 through D.18 are the relationships defining the base coefficient of discharge and the factors used to adjust for nonstandard conditions. Except for type 1 openings, different curves are required for different embankment slopes. Most of these relationships are incorporated into HEC-RAS in the form of digitized values. The digitized values are shown in tabular form at the end of this appendix. Table D.1 cross-references the figures and tables pertaining to the base coefficient of discharge. Table D.2 cross-references those figures and tables pertaining to the various adjustment factors.

Generally each of the relationships are incorporated into HEC-RAS in the form of three arrays. Two one-dimensional arrays contain values of the two independent variables (the abscissa of the relationship and the family of curves), and a two-dimensional array contains the corresponding values of the dependent variable. Exceptions to this form of representation are discussed in the following paragraphs.

The type 1 opening Froude number adjustment (fig. D.8(b)) is adequately expressed in equation form as:

$$k_F = 0.9 + 0.2F \quad (\text{for } 0.0 \leq F \leq 0.5) \quad (\text{D-8})$$

and

$$k_F = 0.82 + 0.36F \quad (\text{for } F > 0.5) \quad (\text{D-9})$$

Where F is the Froude number with an arbitrary upper limit of $F = 1.2$ for the adjustment. The average depth adjustment for a type 3 opening with 2 to 1 embankment slope is determined by the following equations:

$$k_y = 1.00 + 0.3y \quad (\text{for } 0.0 \leq y \leq 0.20) \quad (\text{D-10})$$

and

$$k_y = 1.02 \pm 0.2\bar{y} \quad (\text{for } \bar{y} > 0.2) \quad (\text{D-11})$$

where $\bar{y} = \frac{y_a + y_b}{2b}$ with $\bar{y} = 0.30$ as an upper Limit.

The type 4 opening wing wall adjustment factor, k_θ , is computed using slopes

of the family of curves (figs. D.15 and D.16). The equation for specified m-values is:

$$k_{\theta} = 1.0 + (WW - 30)Sk_{\theta} \quad (D-12)$$

Where WW is the wing wall angle and Sk_{θ} is the appropriate slope from tables D.16 or D.18. k_{θ} is obtained by interpolation for intermediate m-values.

Certain adjustments presented by Matthai were not incorporated into the WSPRO bridge methodology. The skew adjustment was omitted because WSPRO always computes the flow area normal to the flow for skewed bridge openings. An adjustment for submerged flow was also omitted because the FHWA methodology is used to compute pressure flow when girders are significantly submerged. The Froude number adjustment for type 4 openings with 2 to 1 embankment slope was intentionally omitted for reasons of consistency. There is no similar adjustment for type 4 openings with 1 to 1 embankment slopes, and the adjustment is rather minor. Matthai also applied an adjustment for eccentricity, which is a measure of unequal conveyances on left and right overbanks of the approach section. This factor was not included in WSPRO on the bases that (1) it is a very minor adjustment, and (2) the effective flow length accounts for conveyance distribution.

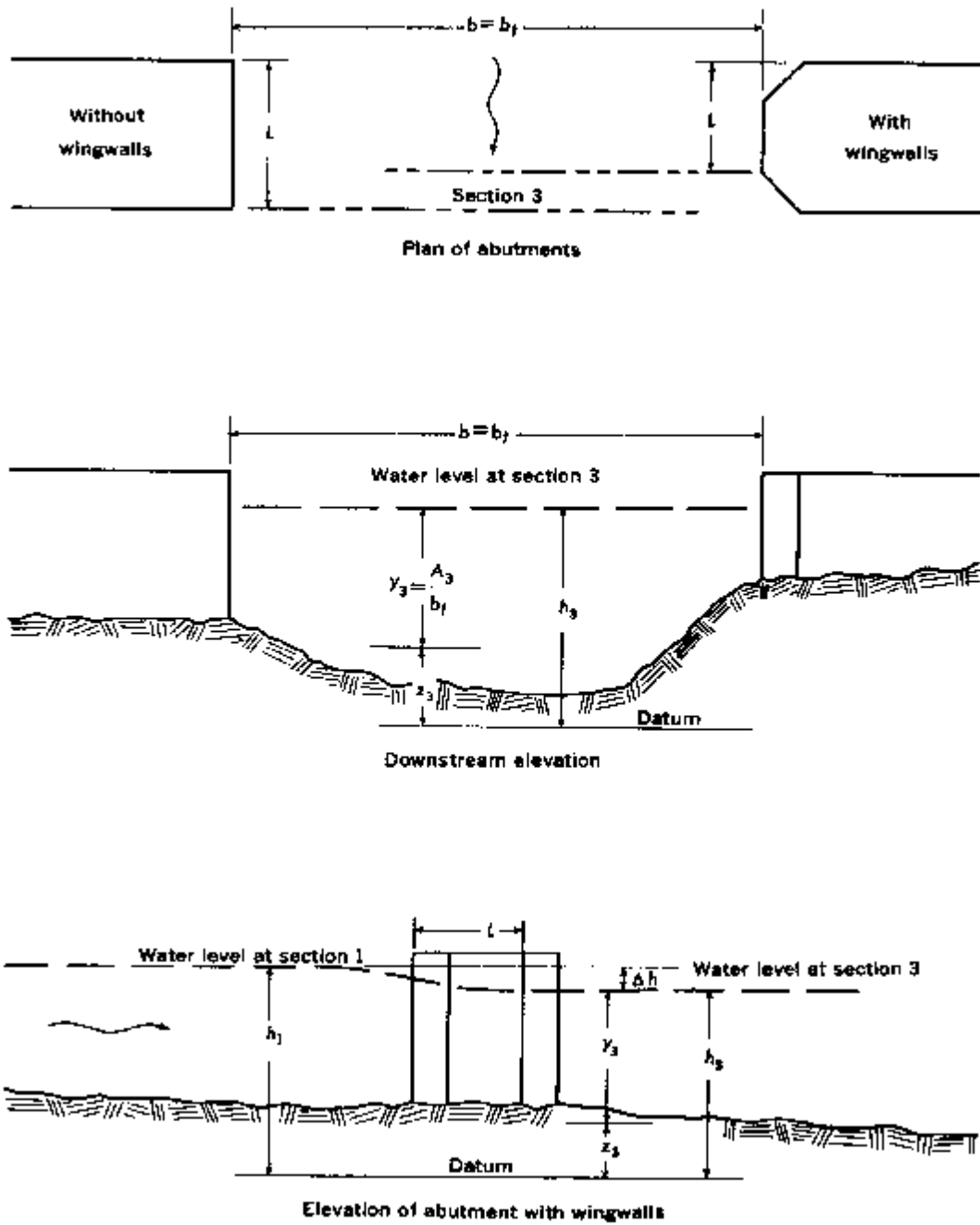


Figure D.4. Definition sketch of type 1 opening, vertical embankments and vertical abutments, with or without wing walls (after Matthai).

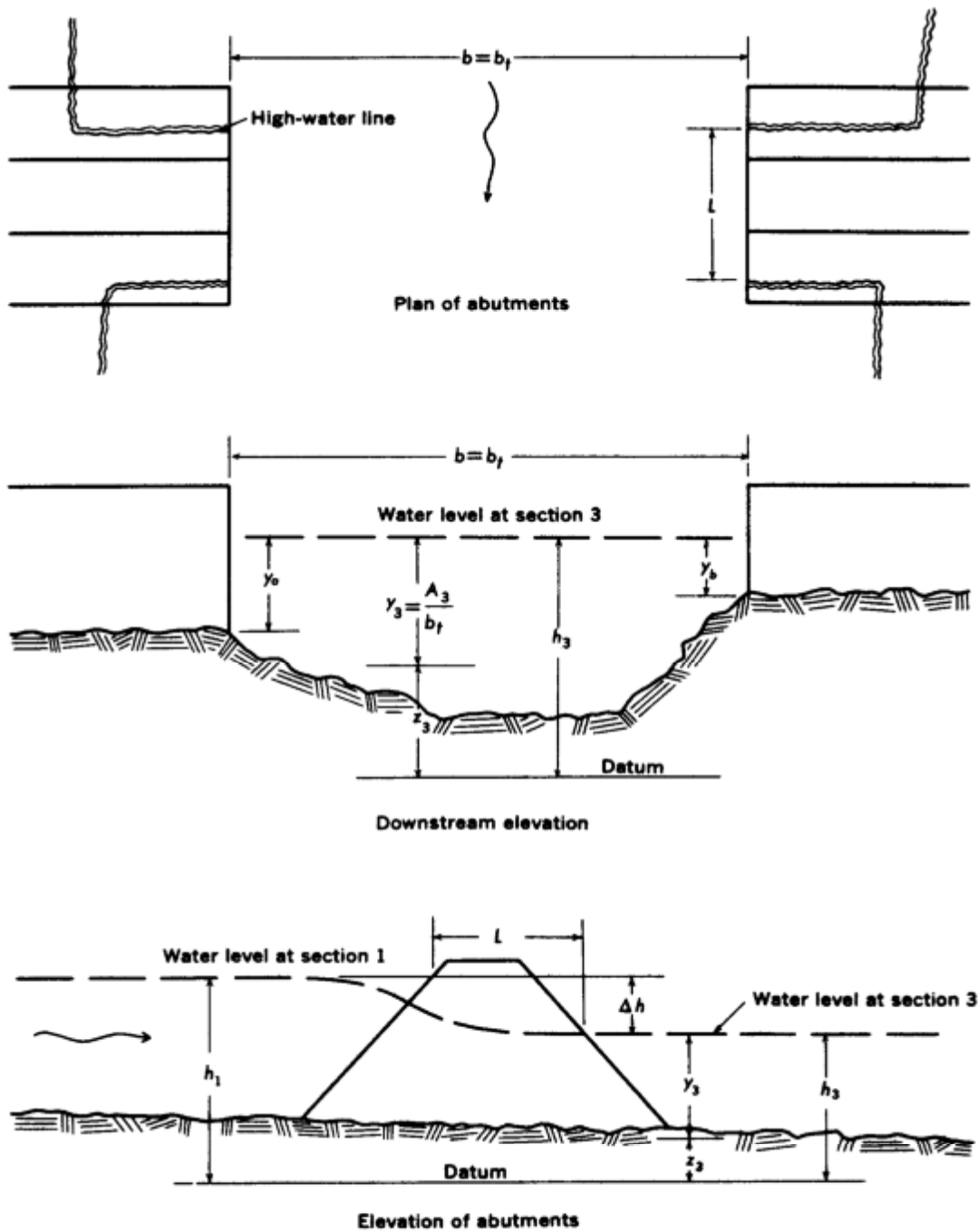


Figure D.5. Definition sketch of type 2 opening, sloping embankments without wing walls (after Matthai).

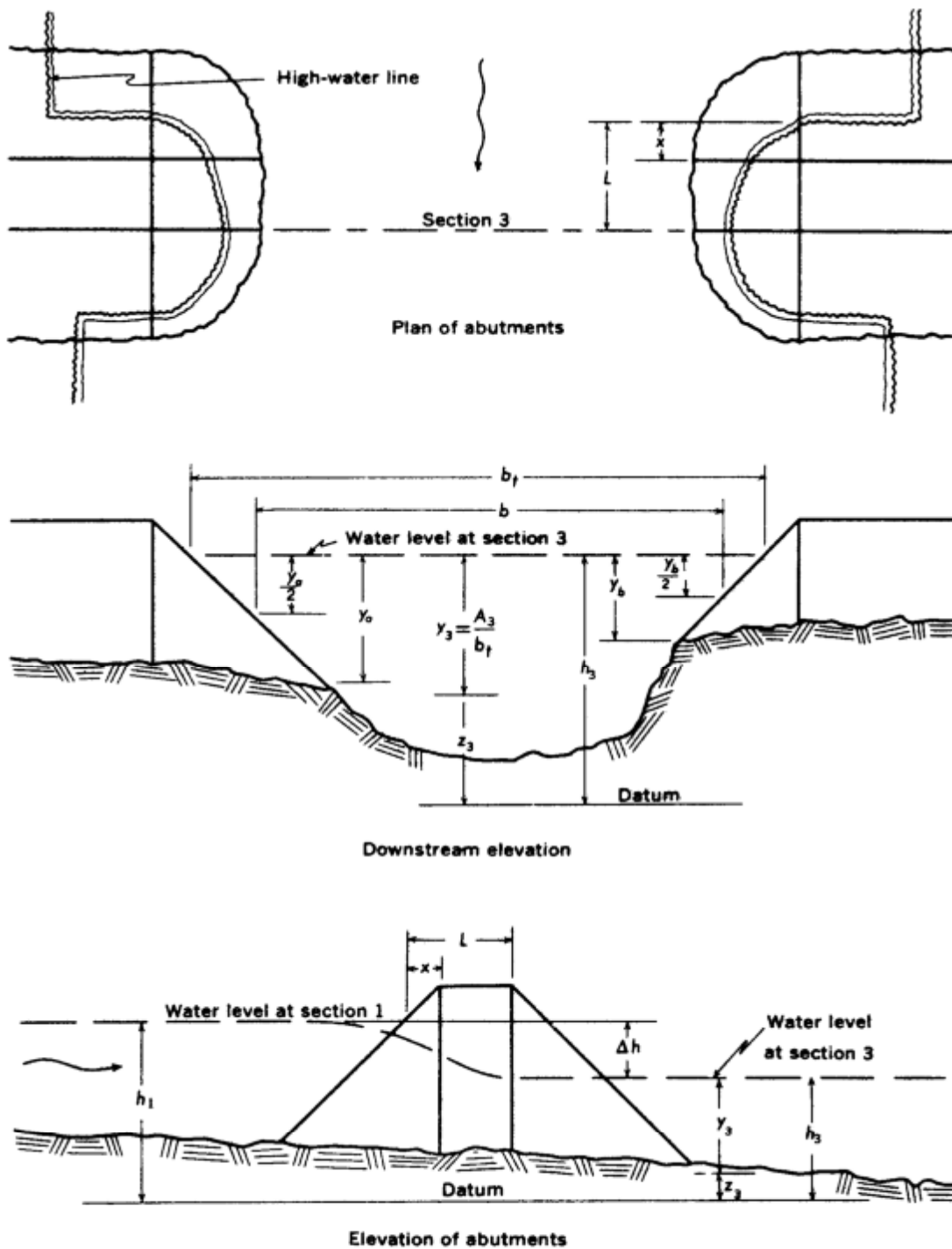


Figure D.6. Definition sketch of type 3 opening, sloping embankments and sloping abutments (spill through) (after Matthai).

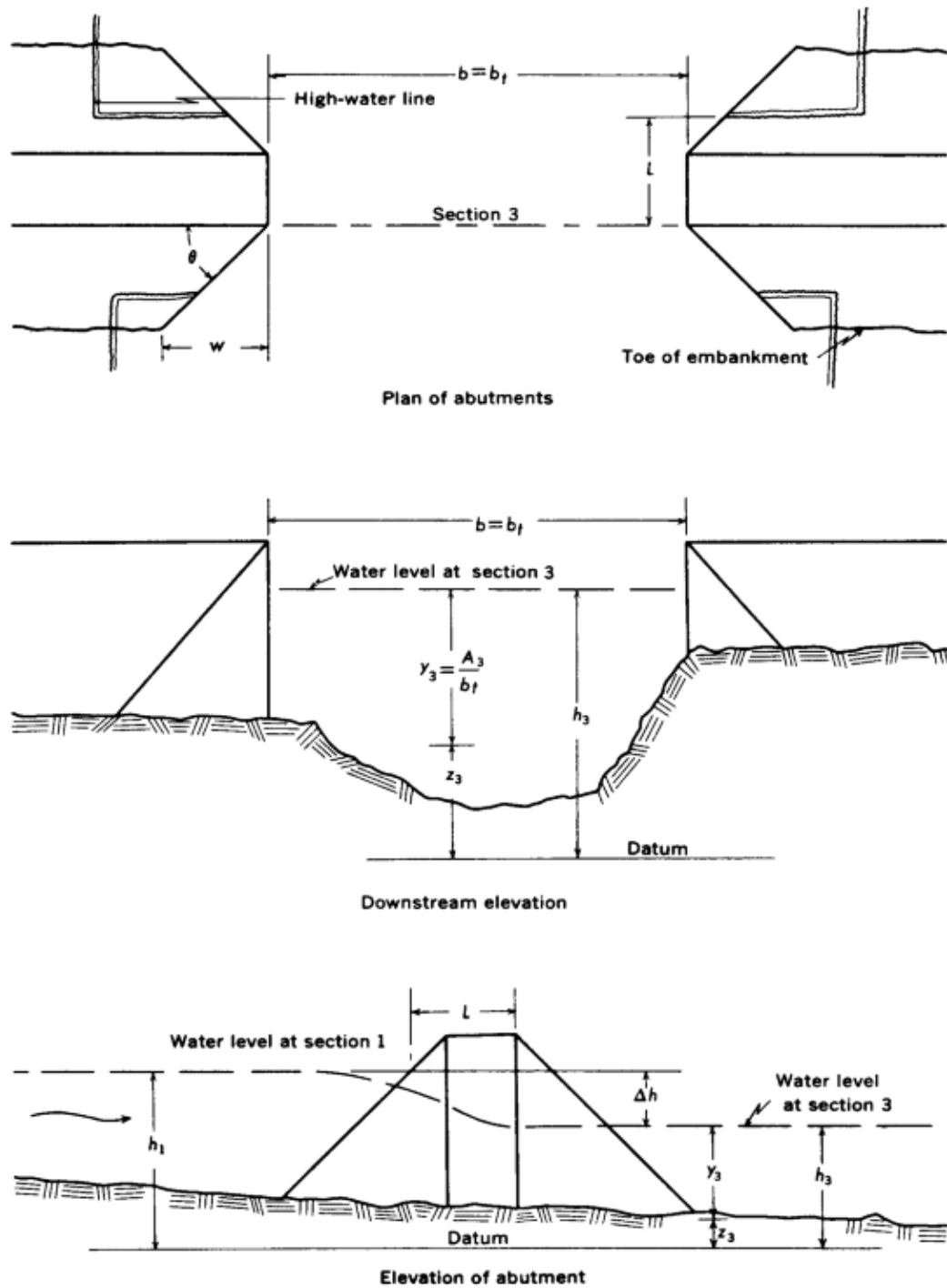


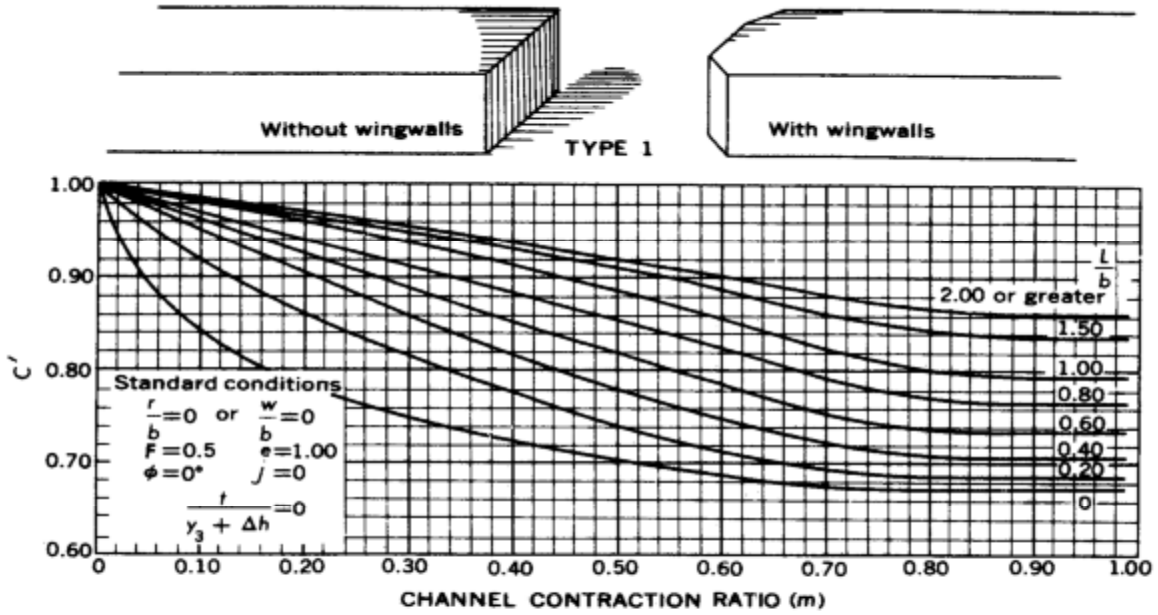
Figure D.7. Definition sketch of type 4 opening, sloping embankments and vertical abutments with wing walls (after Matthai).

Table D.1 Cross-reference of Figures and Tables pertaining to the base coefficient of discharge.

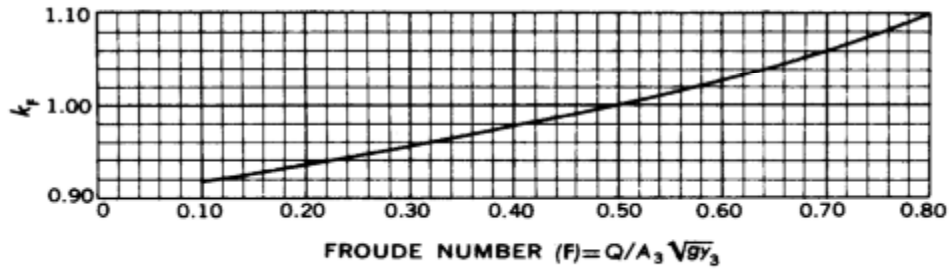
Type Opening	Embankment Slope	Figure No.	Table No.
1		D-8	D-3
2	1 to 1 2 to 1	D-10 D-11	D-6 D-8
3	1 to 1 1 2 to 1 2 to 1	D-12 D-13 D-14	D-10 D-12 D-14
4	1 to 1 2 to 1	D-15 D-16	D-15 D-17

Table D.2 Cross-reference of Figures and Tables pertaining to adjustment factors

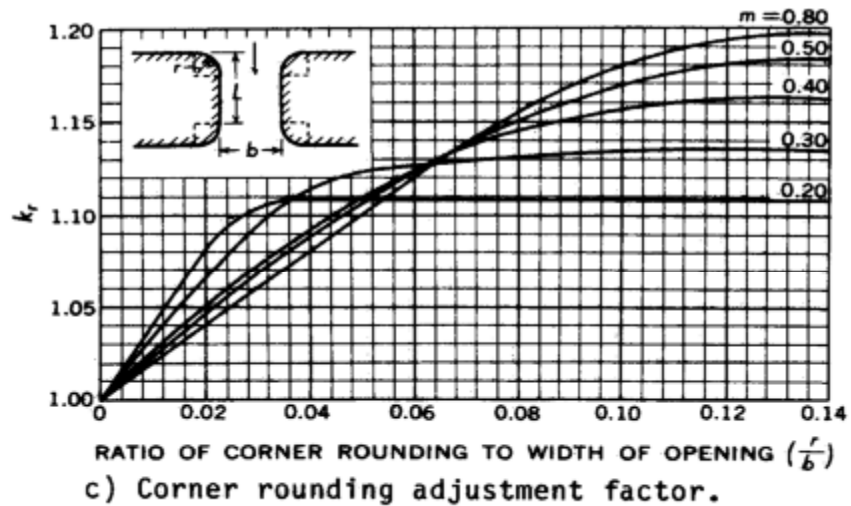
Type Opening	Embankment Slope	Adjustment Factor For:	Figure No.	Table No.
1		Entrance Rounding Wingwalls Froude Number	D-8 D-9 Eqn.	D-4 D-5 Eqn.
2	1 to 1 2 to 1	Average Depth A	D-10 D-11	D-7 D-9
3	1 to 1 1 2 to 1 2 to 1	Entrance Geometry A A	D-12 D-13 Eqn.	D-11 D-13 Eqn.
4	1 to 1 2 to 1	Wingwalls A	D-15 D-16	D-16 D-18
All		Piers or Piles Spur Dikes	D-17 D-18	D-19, D-20 D-21



a) Base coefficient of discharge.



b) Froude number adjustment factor.



c) Corner rounding adjustment factor.

Figure D.8. Coefficients for type 1 openings (after Matthai).

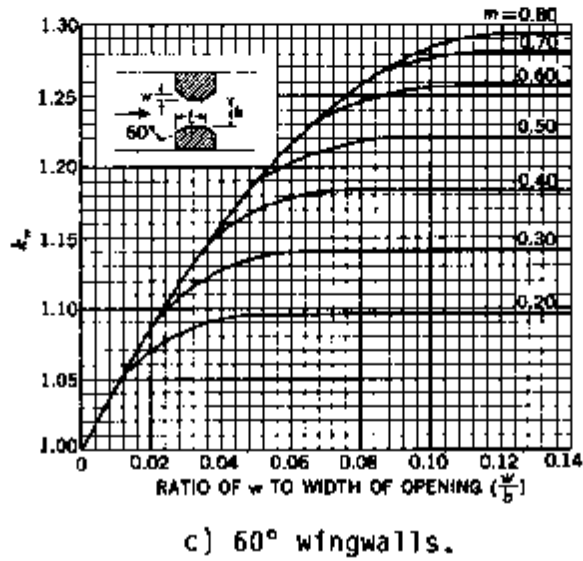
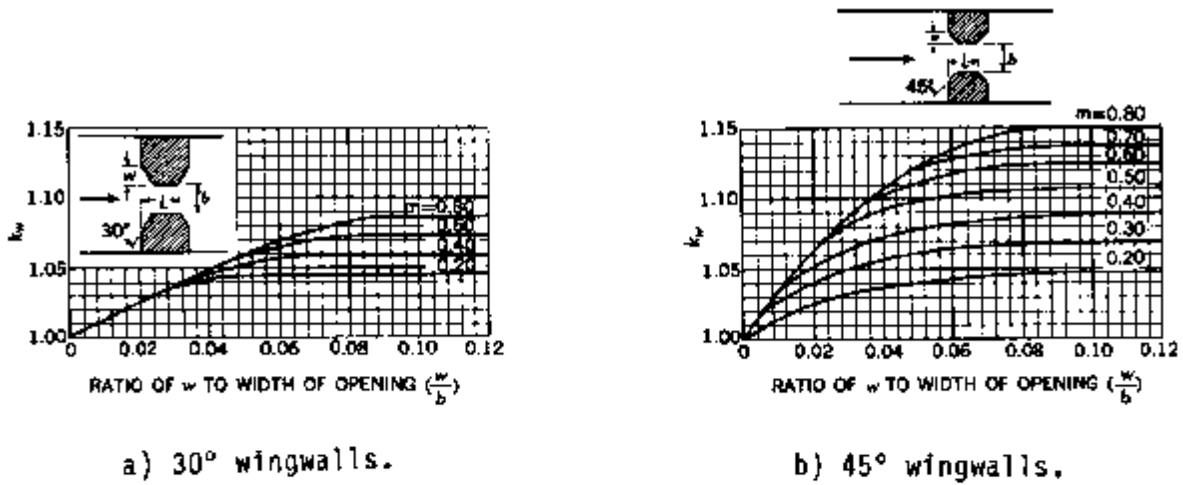
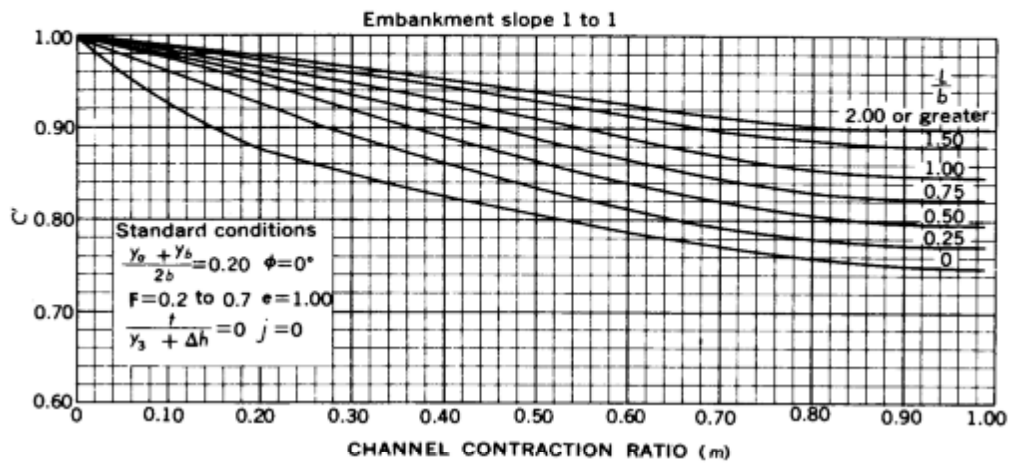
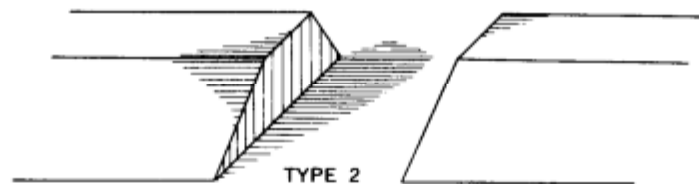
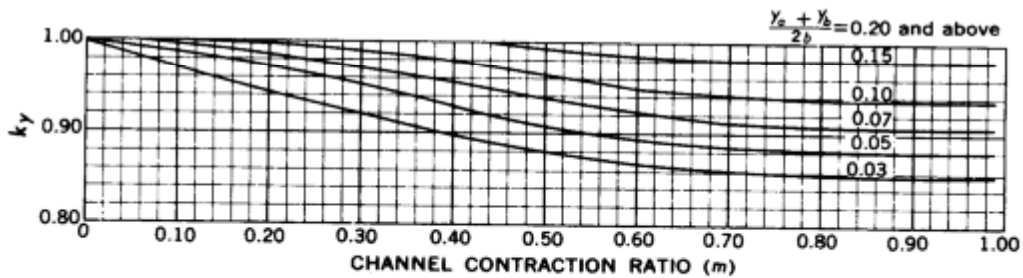


Figure D.9. Wingwall adjustment factors for type 1 openings (after Matthai).

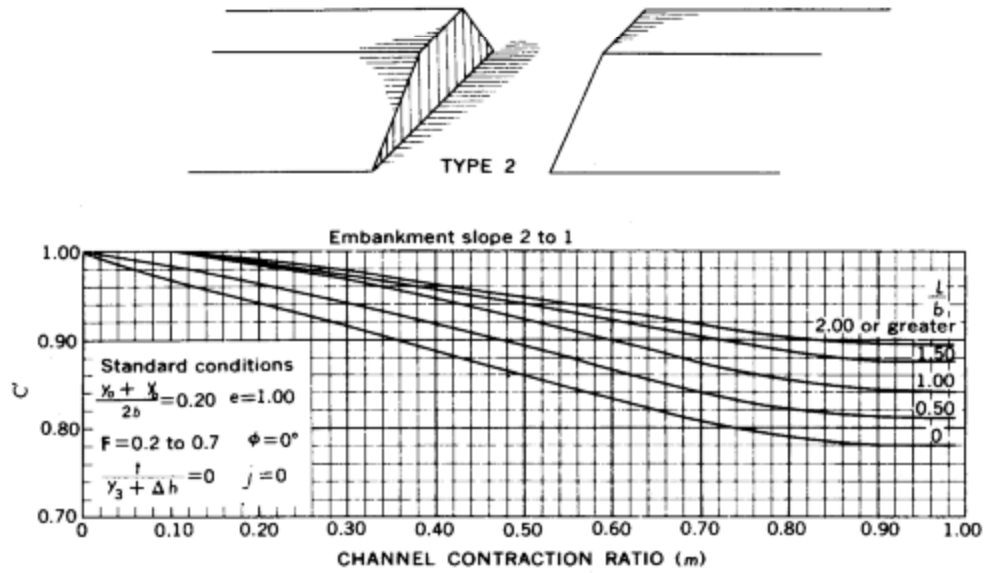


a) Base coefficient of discharge.

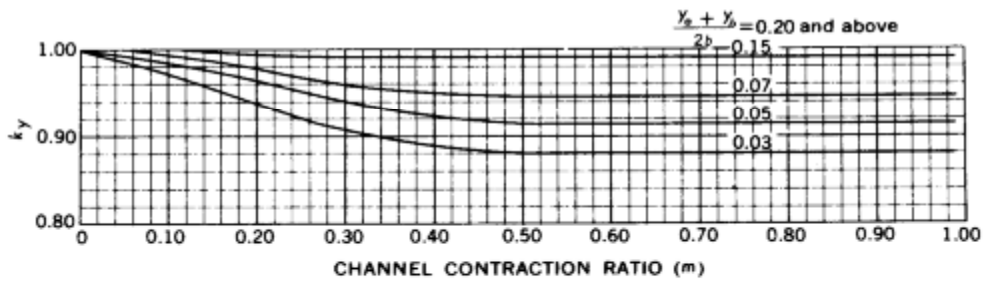


b) Average depth adjustment factor.

Figure D.10. Coefficients for type 2 openings, embankment slope 1 to 1 (after Matthai).

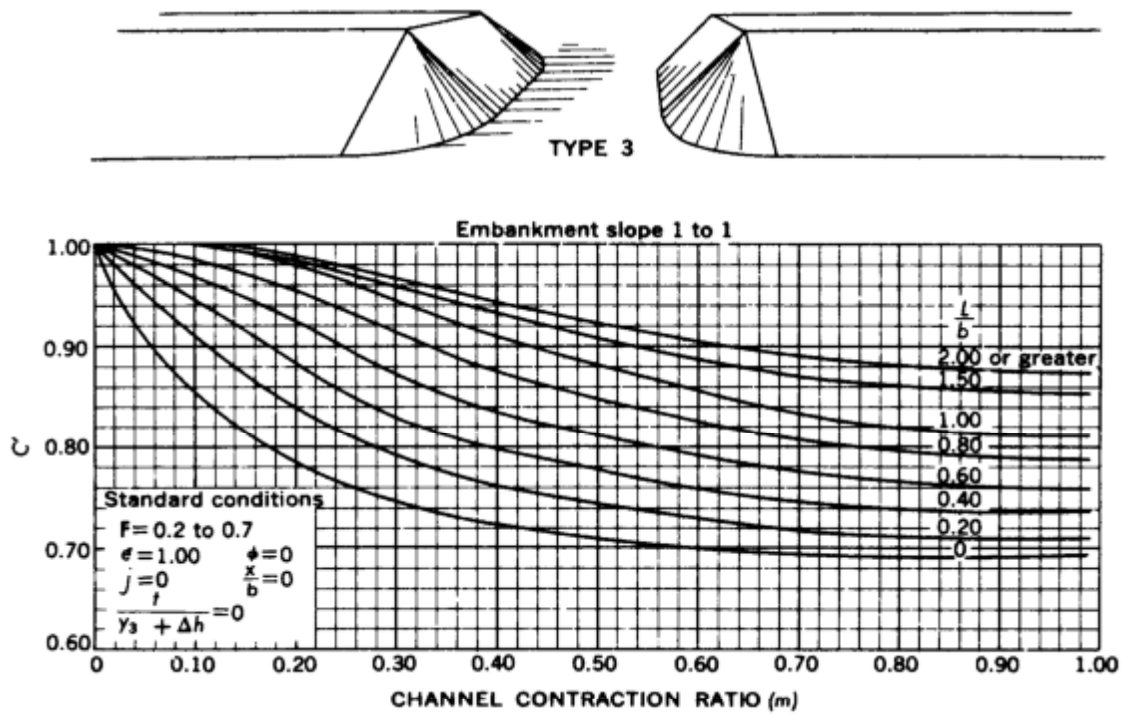


a) Base coefficient of discharge.

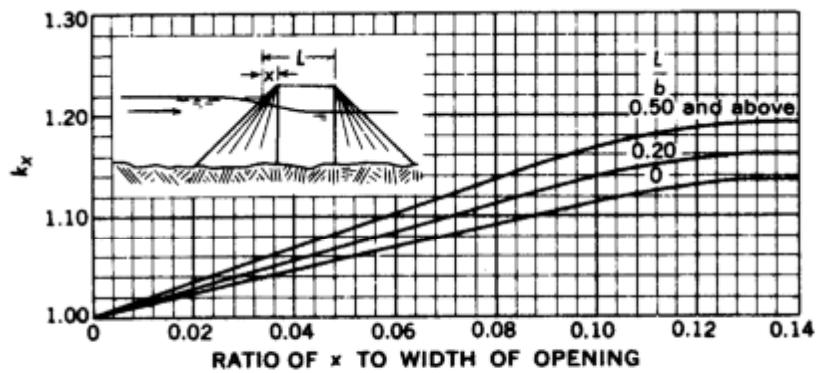


b) Average depth adjustment factor.

Figure D.11. Coefficients for type 2 openings, embankment slope 2 to 1 (after Matthai).

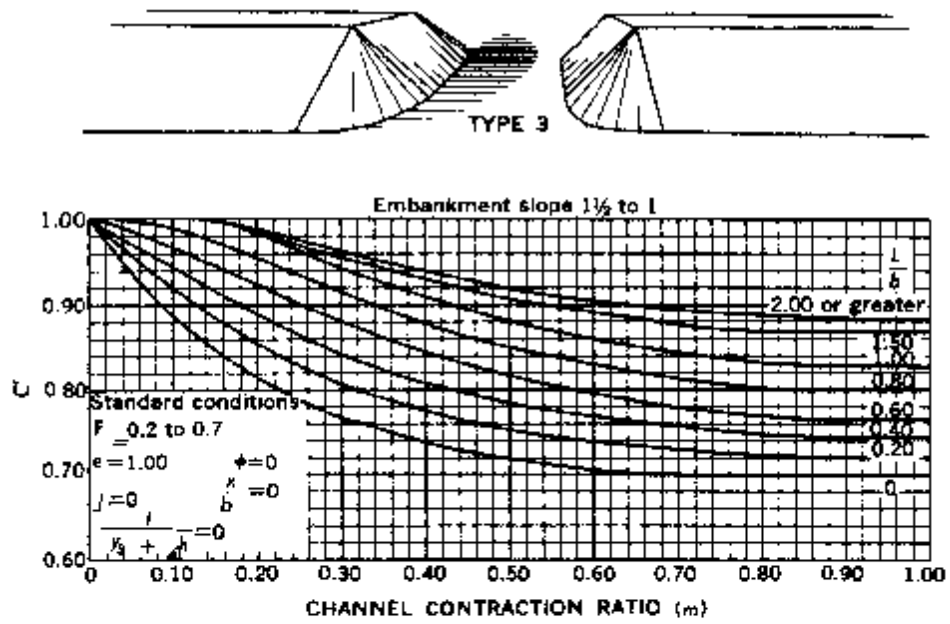


a) Base coefficient of discharge.

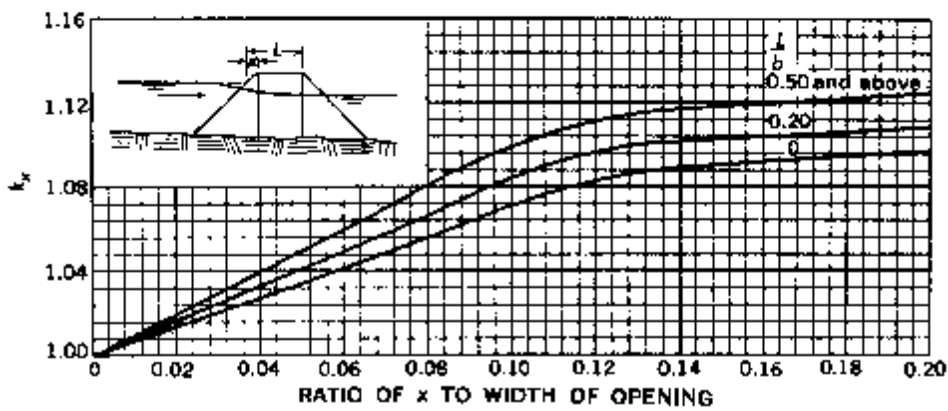


b) Unwetted abutment adjustment factor.

Figure D.12 Coefficients for type 3 openings, embankment slope 1 to 1 (after Matthai).

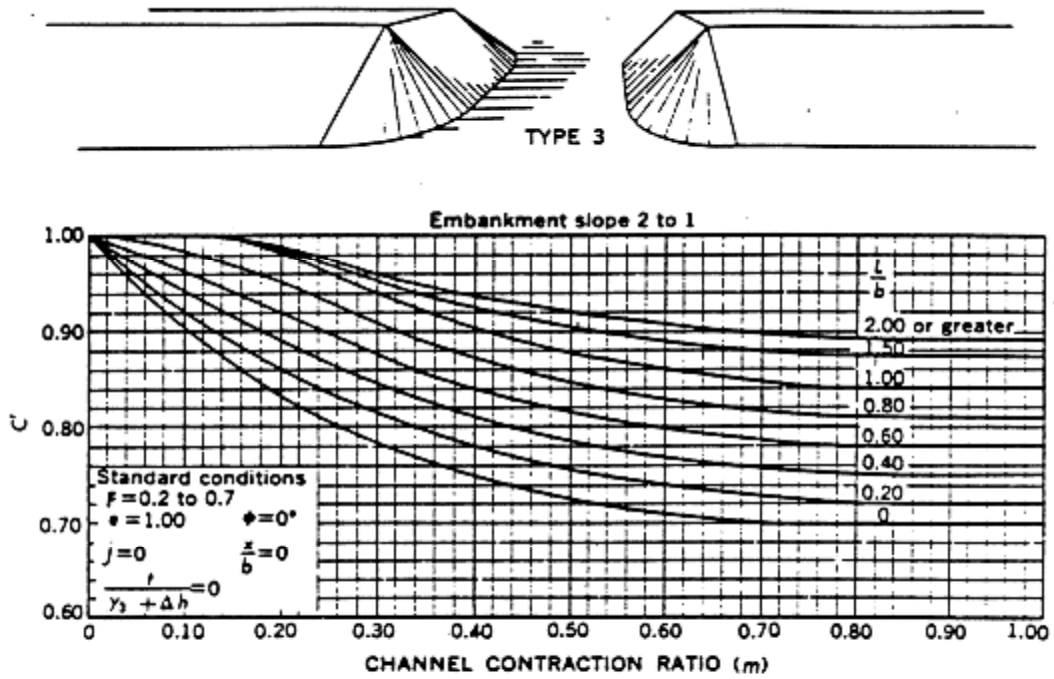


a) Base coefficient of discharge.

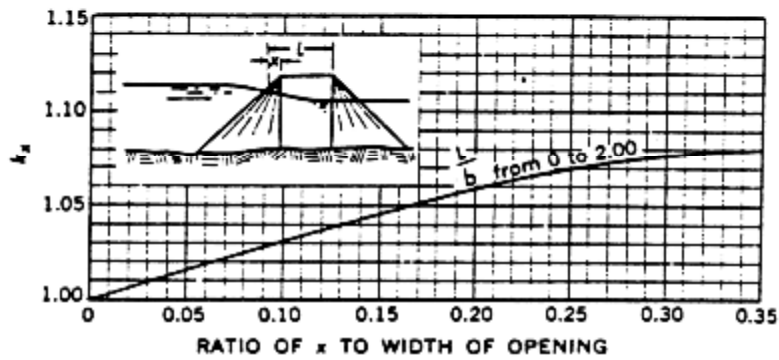


b) Unwetted abutment adjustment factor.

Figure D.13. Coefficients for type 3 openings, embankment slope 1-1/2 to 1 (after Matthai).

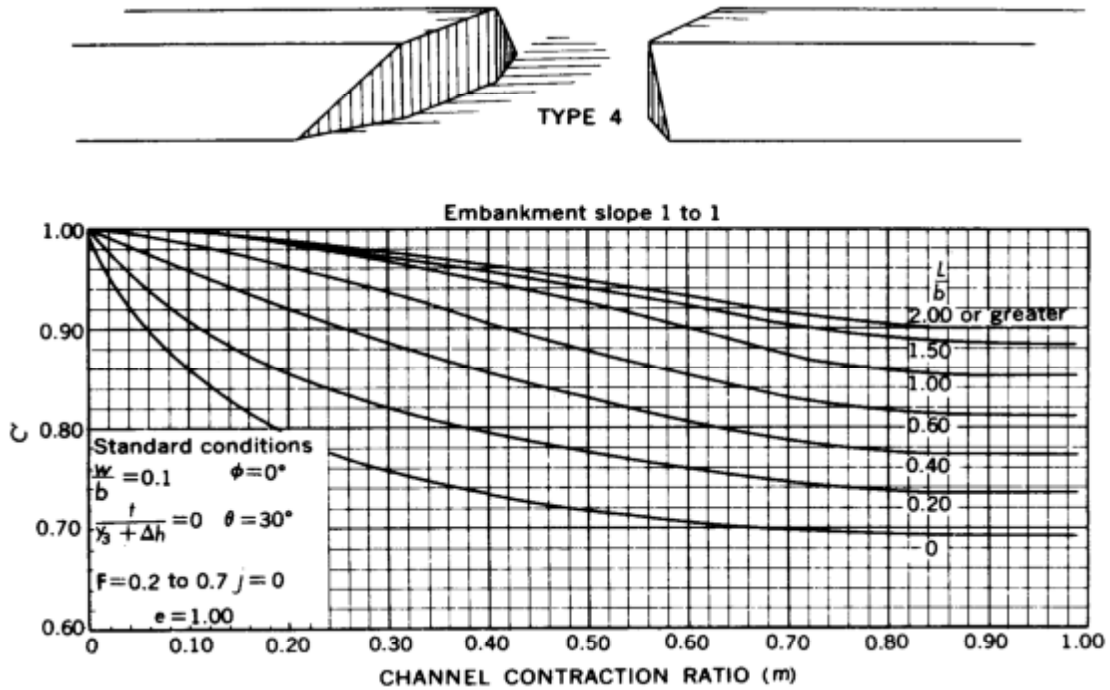


a) Base coefficient of discharge.

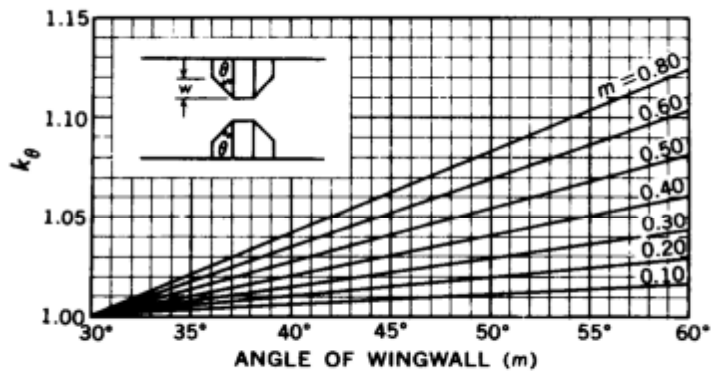


b) Unwetted abutment adjustment factor.

Figure D.14 Coefficients for type 3 openings, embankment slope 2 to 1 (after Matthai)

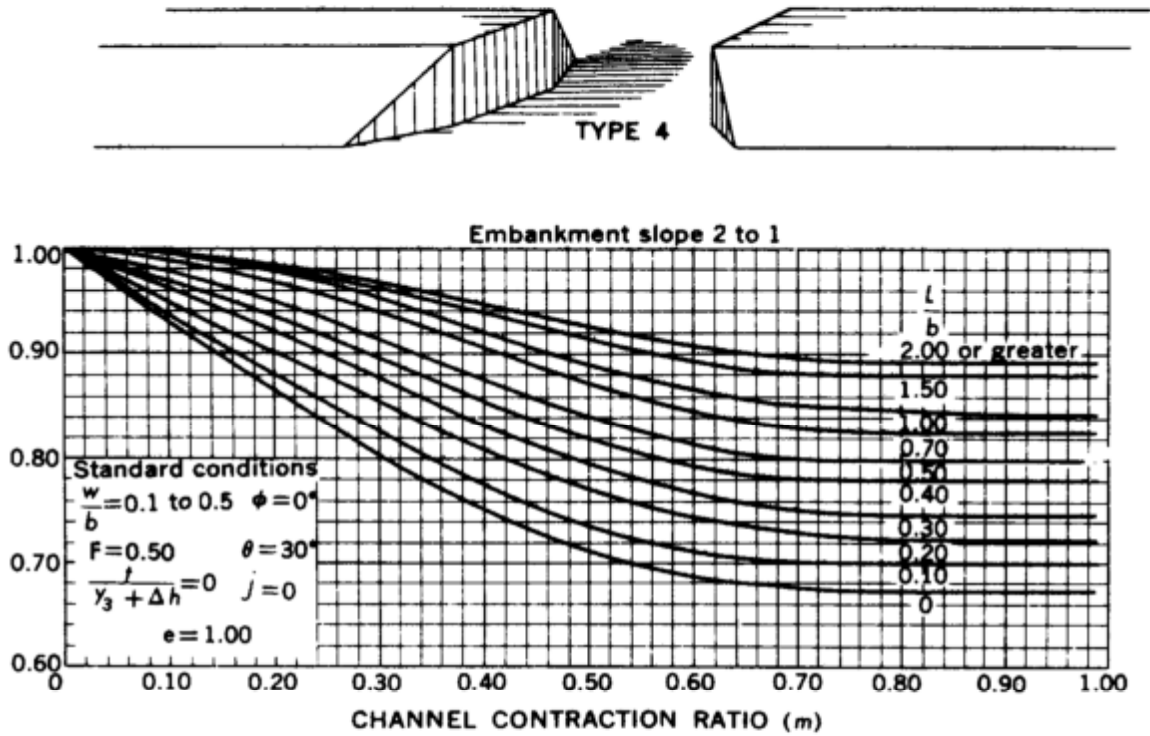


a) Base coefficient of discharge.

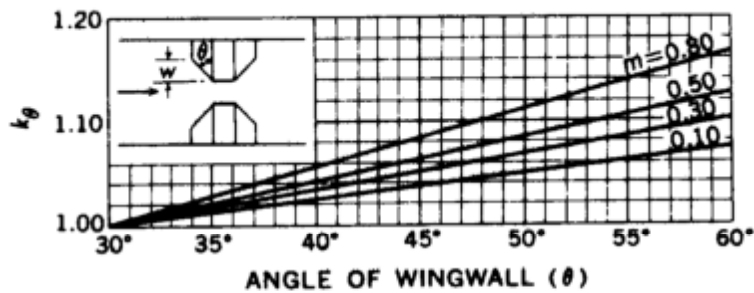


b) Wingwall adjustment factor.

Figure D.15. Coefficients for type 4 openings, embankment slope 1 to 1 (after Matthai).

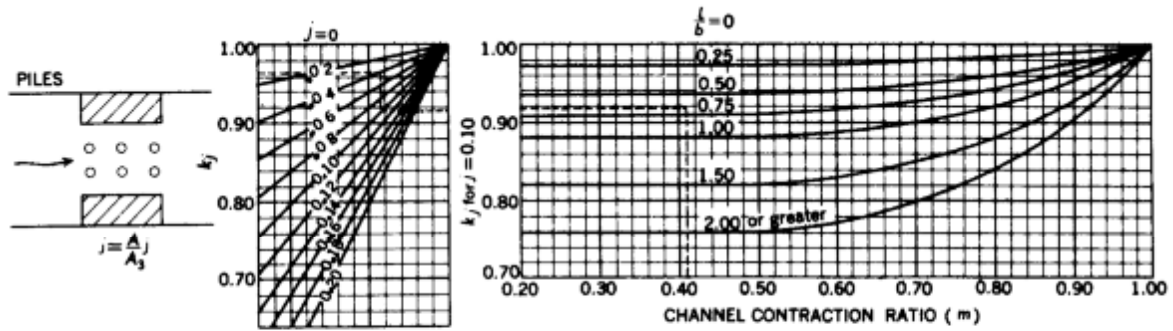


a) Base coefficient of discharge.

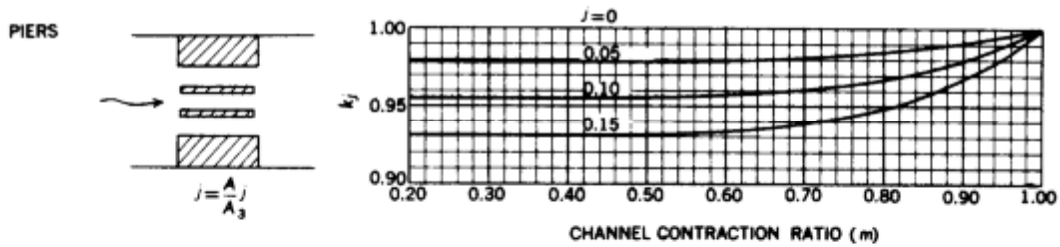


b) Wingwall adjustment factor.

Figure D.16. Coefficients for type 4 openings, embankment slope 2 to 1 (after Matthai).



a) Adjustment factor for piles.



b) Adjustment factor for piers.

Figure D.17. Adjustment factors for piers or piles, all opening types (after Matthai).

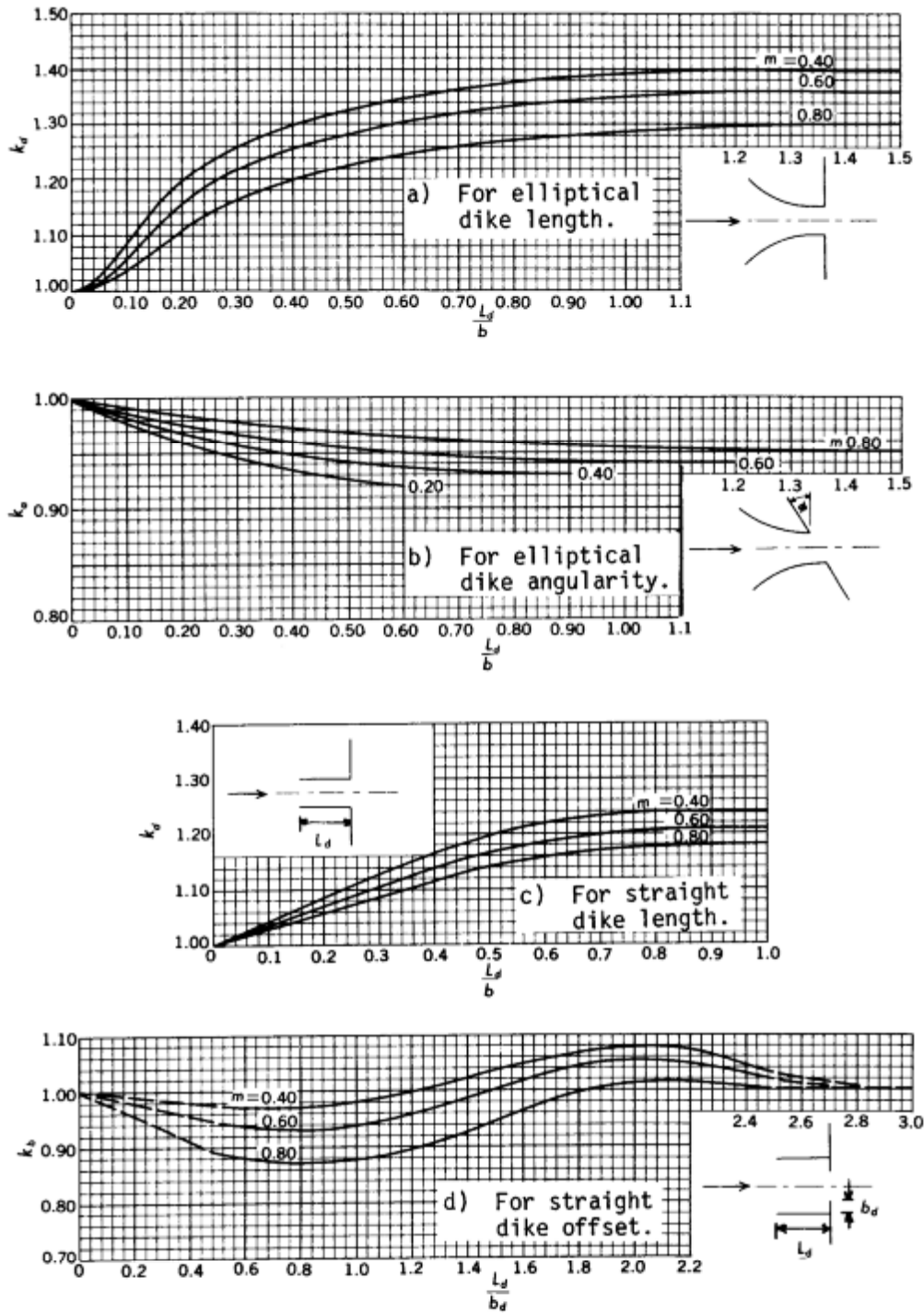


Figure D.18. Adjustment factors for spur dikes, all opening types (after Matthai)

Table D.3 Base coefficient of discharge, C' , for type 1 opening, with or without wing walls (see fig. D-8)

		m					
		0.0	0.1	0.3	0.5	0.8	1.0
L/b	0.0	1.00	0.83	0.745	0.70	0.67	0.67
	0.2	1.00	0.92	0.81	0.74	0.685	0.685
	0.4	1.00	0.95	0.86	0.755	0.71	0.71
	0.6	1.00	0.965	0.89	0.82	0.735	0.735
	0.8	1.00	0.97	0.91	0.855	0.77	0.765
	1.0	1.00	0.98	0.935	0.885	0.80	0.795
	1.5	1.00	0.985	0.95	0.91	0.845	0.835
	2.0	1.00	0.99	0.955	0.92	0.87	0.86

m is the channel contraction ratio.

L/b is the ratio of flow length to bridge-opening width.

Table D.4 Variation of adjustment factor, k_r , for type 1 opening with entrance rounding (see fig. D-8).

		r/b						
		0.01	0.02	0.04	0.06	0.08	0.10	0.14
m	0.1	1.06	1.07	1.07	1.07	1.07	1.07	1.07
	0.2	1.04	1.08	1.11	1.11	1.11	1.11	1.11
	0.4	1.03	1.05	1.09	1.12	1.14	1.15	1.16
	0.6	1.02	1.04	1.08	1.12	1.15	1.17	1.18
	0.8	1.02	1.04	1.08	1.12	1.16	1.18	1.20
	1.0	1.02	1.04	1.08	1.12	1.16	1.18	1.22

r/b is the ratio of entrance rounding to bridge-opening width.

m is the channel contraction ratio.

Table D.5. Variation of adjustment factor, k_0 , for type 1 opening with wing walls (fig. D-9).

w/b

	0.01	0.02	0.04	0.06	0.08	0.10	0.14
0.1	1.01	1.02	1.02	1.02	1.02	1.02	1.02
0.2	1.01	1.025	1.04	1.04	1.04	1.04	1.04
m 0.4	1.01	1.025	1.04	1.06	1.06	1.06	1.06
0.6	1.01	1.025	1.05	1.06	1.07	1.07	1.07
0.8	1.01	1.025	1.05	1.07	1.08	1.09	1.09
1.0	1.01	1.025	1.05	1.07	1.08	1.09	1.10

(a) 30° wing walls

	0.01	0.02	0.04	0.06	0.08	0.10	0.14
0.1	1.00	1.01	1.01	1.02	1.02	1.02	1.02
0.2	1.01	1.02	1.04	1.04	1.05	1.05	1.05
m 0.4	1.03	1.05	1.07	1.08	1.09	1.09	1.09
0.6	1.03	1.06	1.10	1.11	1.12	1.12	1.12
0.8	1.03	1.06	1.11	1.13	1.15	1.15	1.15
1.0	1.03	1.06	1.11	1.13	1.15	1.16	1.17

(b) 45° wing walls

	0.01	0.02	0.04	0.06	0.08	0.10	0.14
0.1	1.02	1.04	1.05	1.05	1.05	1.05	1.05
0.2	1.04	1.07	1.09	1.10	1.10	1.10	1.10
m 0.4	1.04	1.09	1.15	1.18	1.18	1.18	1.18
0.6	1.04	1.09	1.15	1.21	1.24	1.25	1.26
0.8	1.04	1.09	1.15	1.22	1.26	1.28	1.29
1.0	1.04	1.09	1.15	1.22	1.26	1.28	1.32

(c) 60° wingwalls

w/b is the ratio of wing wall width to bridge-opening width.

Table D.6 Base coefficient of discharge, C' , for type 2 opening, embankment slope 1 to 1 (see fig. D-10).

m		0.0	0.1	0.3	0.5	0.8	1.0
0.0		1.00	0.92	0.845	0.805	0.755	0.745
0.2		1.00	0.955	0.88	0.83	0.775	0.765
0.4		1.00	0.97	0.91	0.85	0.795	0.79
L/b	0.6	1.00	0.975	0.925	0.87	0.81	0.805
	0.8	1.00	0.98	0.94	0.895	0.835	0.825
	1.0	1.00	0.985	0.95	0.91	0.855	0.845
	1.5	1.00	0.988	0.96	0.93	0.885	0.88
	2.0	1.00	0.99	0.965	0.94	0.905	0.90

m is the channel contraction ratio.

L/b is the ratio of flow length to bridge-opening width.

Table D.7 Variation of adjustment factor, k_y , for type 2 opening, embankment slope 1 to 1 (see fig. D-10).

m		0.0	0.2	0.4	0.7	1.0
$y_a + y_b$	0.03	1.00	0.94	0.895	0.86	0.86
-----	0.05	1.00	0.97	0.93	0.88	0.88
2b	0.07	1.00	0.985	0.955	0.91	0.91
	0.10	1.00	0.995	0.98	0.94	0.94
	0.15	1.00	1.00	1.00	0.98	0.98

m is the channel contraction ratio.

$(y_a + y_b)/2b$ is the ratio of average depth at the abutments to bridge-opening width.

Table D.8 Base coefficient of discharge, C' , for type 2 opening, embankment slope 2 to 1 (see fig. D-11).

m	0.0	0.1	0.3	0.5	0.8	1.0
0.0	1.00	0.965	0.915	0.86	0.79	0.78
0.2	1.00	0.97	0.925	0.87	0.80	0.79
0.4	1.00	0.98	0.935	0.89	0.81	0.80
L/b 0.6	1.00	0.99	0.95	0.90	0.83	0.82
0.8	1.00	0.995	0.96	0.91	0.845	0.83
1.0	1.00	1.00	0.97	0.925	0.855	0.84
1.5	1.00	1.00	0.975	0.94	0.89	0.875
2.0	1.00	1.00	0.98	0.95	0.905	0.895

m is the channel contraction ratio.

L/b is the ratio of flow length to bridge-opening width.

Table D.9 Variation of adjustment factor, k , for type 2 opening, embankment slope 2 to 1 (see fig. D-11).

m		0.0	0.2	0.4	0.7	1.0
$\frac{y_a + y_b}{2b}$	0.03	1.00	0.935	0.89	0.88	0.88
	0.05	1.00	0.965	0.925	0.91	0.91
	0.07	1.00	0.975	0.95	0.945	0.945
	0.10	1.00	0.985	0.97	0.97	0.97
	0.15	1.00	0.99	0.99	0.99	0.99

m is the channel contraction ratio.

$(y_a + y_b)/2b$ is the ratio of average depth at the abutments to bridge-opening width.

Table D.10 Base coefficient of discharge, C' , for type 3 opening, embankment slope 1 to 1 (see fig. D-12).

	m					
	0.0	0.1	0.3	0.5	0.8	1.0
0.0	1.00	0.85	0.74	0.71	0.69	0.69
0.2	1.00	0.91	0.79	0.745	0.71	0.71
0.4	1.00	0.945	0.83	0.775	0.74	0.735
L/b 0.6	1.00	0.97	0.87	0.81	0.765	0.76
0.8	1.00	0.985	0.91	0.85	0.795	0.79
1.0	1.00	0.995	0.945	0.88	0.82	0.81
1.5	1.00	1.00	0.96	0.91	0.86	0.85
2.0	1.00	1.00	0.97	0.925	0.88	0.875

m is the channel contraction ratio.

L/b is the ratio of flow length to bridge-opening width.

Table D.11 Variation of adjustment factor, k_y , for type 3 opening, embankment slope 1 to 1 (see fig. D-12).

	x/b					
	0.00	0.08	0.12	0.16	0.20	0.25
0.0	1.00	1.09	1.13	1.14	1.14	1.14
L/b 0.2	1.00	1.11	1.155	1.16	1.16	1.16
0.5	1.00	1.135	1.19	1.20	1.20	1.20

x/b is the ratio of "unwetted" abutment length to bridge-opening width.

L/b is the ratio of flow length to bridge-opening width.

Table D.12 Base coefficient of discharge, C' , for type 3 opening, embankment slope 1-1/2 to 1 (see fig. D-13).

	m					
	0.0	0.1	0.3	0.5	0.8	1.0
0.0	1.00	0.885	0.76	0.715	0.70	0.70
0.2	1.00	0.92	0.80	0.75	0.725	0.72
0.4	1.00	0.945	0.84	0.78	0.75	0.745
L/b 0.6	1.00	0.97	0.88	0.815	0.77	0.765
0.8	1.00	0.99	0.915	0.85	0.805	0.80
1.0	1.00	1.00	0.945	0.88	0.83	0.825
1.5	1.00	1.00	0.955	0.905	0.87	0.87
2.0	1.00	1.00	0.965	0.92	0.885	0.885

m is the channel contraction ratio.

L/b is the ratio of flow length to bridge-opening width.

Table D.13 Variation of adjustment factor, k_x , for type 3 opening, embankment slope 1-1/2 to 1 (see fig. D-13).

	x/b					
	0.00	0.08	0.12	0.16	0.20	0.25
0.0	1.00	1.055	1.085	1.09	1.095	1.10
L/b 0.2	1.00	1.065	1.10	1.105	1.11	1.115
0.5	1.00	1.08	1.11	1.12	1.125	1.13

x/b is the ratio of "unwetted" abutment length to bridge-opening width.

L/b is the ratio of flow length to bridge-opening width.

Table D.14 Base coefficient of discharge, C' , for type 3 opening, embankment slope 2 to 1 (see fig. D-14).

	m					
	0.0	0.1	0.3	0.5	0.8	1.0
0.0	1.00	0.90	0.78	0.72	0.70	0.70
0.2	1.00	0.92	0.81	0.755	0.72	0.72
0.4	1.00	0.94	0.845	0.785	0.75	0.75
L/b 0.6	1.00	0.96	0.875	0.81	0.78	0.78
0.8	1.00	0.985	0.91	0.845	0.81	0.81
1.0	1.00	1.00	0.94	0.87	0.845	0.84
1.5	1.00	1.00	0.95	0.905	0.875	0.87
2.0	1.00	1.00	0.96	0.92	0.895	0.89

m is the channel contraction ratio.

L/b is the ratio of flow length to bridge-opening width.

Table D.15 Base coefficient of discharge, C' , for type 4 opening, embankment slope 1 to 1 (see fig. D-15).

	m					
	0.0	0.1	0.3	0.5	0.8	1.0
0.0	0.99	0.85	0.755	0.715	0.695	0.69
0.2	1.00	0.90	0.815	0.775	0.735	0.73
0.4	1.00	0.955	0.885	0.83	0.775	0.77
L/b 0.6	1.00	0.985	0.935	0.875	0.815	0.81
0.8	1.00	0.99	0.955	0.91	0.84	0.835
1.0	1.00	1.00	0.965	0.925	0.855	0.85
1.5	1.00	1.00	0.97	0.94	0.89	0.885
2.0	1.00	1.00	0.975	0.95	0.905	0.90

m is the channel contraction ratio.

L/b is the ratio of flow length to bridge-opening width.

Table D.16 Slopes of family of curves for determining adjustment factor, k_0 , for wing wall Angle for type 4 openings, embankment slope 1 to 1 (see fig. D-15).

m	Sk_0
0.1	0.00057
0.2	0.001
0.4	0.002
0.6	0.00343
0.8	0.00413
1.0	0.00483

Table D.17 Base coefficient of discharge, C' , for type 4 opening, embankment slope 2 to 1 (see fig. D-16).

	m					
	0.0	0.1	0.3	0.5	0.8	1.0
0.0	1.00	0.93	0.80	0.705	0.67	0.67
0.2	1.00	0.95	0.855	0.765	0.725	0.725
0.4	1.00	0.97	0.895	0.815	0.78	0.78
L/b 0.6	1.00	0.985	0.925	0.845	0.805	0.805
0.8	1.00	0.99	0.94	0.87	0.825	0.825
1.0	1.00	0.995	0.95	0.89	0.85	0.85
1.5	1.00	0.995	0.965	0.91	0.88	0.88
2.0	1.00	1.00	0.97	0.925	0.89	0.89

m is the channel contraction ratio.

L/b is the ratio of flow length to bridge-opening width.

Table D.18 Slopes of family of curves for determining adjustment factor, k_0 , for wing wall Angle for type 4 openings, embankment slope 2 to 1 (see fig. D-16).

m	Sk_0
0.1	0.00243
0.2	0.00283
0.4	0.00373
0.6	0.00467
0.8	0.00557
1.0	0.00667

Table D.19 Adjustment factor, k_j , for piers (see fig. D-17).

		m				
		0.40	0.60	0.80	0.90	1.00
	0.00	1.00	1.00	1.00	1.00	1.00
	0.05	0.978	0.979	0.985	0.991	1.00
j	0.10	0.955	0.957	0.967	0.98	1.00
	0.15	0.93	0.933	0.948	0.968	1.00
	0.20	0.903	0.907	0.928	0.956	1.00

Table D.20 Adjustment factor, k_j , for piles (see fig. 17).

		m				
		0.40	0.60	0.80	0.90	1.00
	0.00	1.00	1.00	1.00	1.00	1.00
	0.25	0.973	0.976	0.984	0.99	1.00
L/b	0.50	0.933	0.94	0.96	0.976	1.00
	1.00	0.88	0.888	0.92	0.953	1.00
	2.00	0.76	0.772	0.84	0.905	1.00

(a) k_j for piles when $j = 0.10$

		j					
		0.00	0.04	0.08	0.12	0.16	0.20
	.76	1.00	0.902	0.81	0.71	0.615	0.52
k_j for	.80	1.00	0.92	0.841	0.761	0.684	0.605
j=.1	.90	1.00	0.961	0.921	0.88	0.842	0.802
	1.0	1.00	1.00	1.00	1.00	1.00	1.00

(b) k_j for piles when $j \text{ @ } 0.10$

Table D.21 Adjustment factors for spur dikes (see fig. D-18).

$L_{d/b}$	0.0	0.2	0.4	0.6	1.0	1.5
0.2	1.00	1.23	1.32	1.37	1.41	1.42
m 0.4	1.00	1.20	1.30	1.35	1.39	1.40
0.6	1.00	1.16	1.25	1.30	1.35	1.36
0.8	1.00	1.11	1.20	1.25	1.29	1.30

(a) K_d for elliptical dike length

$L_{d/b}$	0.0	0.2	0.4	0.6	1.0	1.5
0.2	1.00	0.96	0.935	0.92	0.91	0.905
m 0.4	1.00	0.968	0.95	0.935	0.93	0.925
0.6	1.00	0.976	0.96	0.95	0.94	0.935
0.8	1.00	0.984	0.973	0.965	0.955	0.95

(b) K_a for elliptical dike angularity

$L_{d/b}$	0.0	0.2	0.4	0.6	1.0	1.5
0.2	1.00	1.09	1.18	1.25	1.27	1.27
m 0.4	1.00	1.08	1.16	1.22	1.24	1.24
0.6	1.00	1.07	1.14	1.18	1.21	1.21
0.8	1.00	1.06	1.12	1.16	1.18	1.18

(c) K_d for straight dike length

$L_{d/b}$ d	0.0	0.5	1.0	1.5	2.0	2.8
0.2	1.00	0.99	1.00	1.06	1.10	1.00
m 0.4	1.00	0.97	0.98	1.04	1.08	1.00
0.6	1.00	0.94	0.94	1.00	1.05	1.00
0.8	1.00	0.89	0.88	0.945	1.01	1.00

(d) K_b for straight dike offset